Published in final edited form as:
Mol Cell. 2013 February 7; 49(3): 558–570. doi:10.1016/j.molcel.2012.11.019.

LSD2/KDM1B and Its Cofactor NPAC/GLYR1 Endow a Structural and Molecular Model for Regulation of H3K4 Demethylation

Rui Fang[1,8], **Fei Chen**[2,4,8], **Zhenghong Dong**[2,4], **Di Hu**[1,2], **Andrew J. Barbera**[1], **Erin A. Clark**[1], **Jian Fang**[2,4], **Ying Yang**[2,4], **Pinchao Mei**[1], **Michael Rutenberg**[1], **Ze Li**[2,4], **Ying Zhang**[2,3], **Youwei Xu**[2,4], **Huirong Yang**[2,4], **Ping Wang**[2,4], **Matthew D. Simon**[7], **Qiongjie Zhou**[1,5], **Jing Li**[1], **Mark P. Marynick**[1], **Xiaotian Li**[5], **Haojie Lu**[2,3], **Ursula B. Kaiser**[1], **Robert E. Kingston**[7], **Yanhui Xu**[2,4,*], and **Yujiang Geno Shi**[1,2,6,*]

[1]Division of Endocrinology, Diabetes, and Hypertension, Department of Medicine and Department of Biological Chemistry & Molecular Pharmacology, Brigham and Women's Hospital and Harvard Medical School, 221 Longwood Avenue, Boston, MA 02115, USA

[2]Institutes of Biomedical Sciences Fudan University, 130 Dong An Road, Shanghai 200032, China

[3]Department of Chemistry Fudan University, 130 Dong An Road, Shanghai 200032, China

[4]State Key Laboratory of Genetic Engineering Fudan University, 130 Dong An Road, Shanghai 200032, China

[5]Obstetrics and Gynecology Hospital Fudan University, 130 Dong An Road, Shanghai 200032, China

[6]Children's Hospital Fudan University, 130 Dong An Road, Shanghai 200032, China

[7]Department of Molecular Biology, Massachusetts General Hospital, Boston, MA 02114, USA

SUMMARY

Dynamic regulation of histone methylation represents a fundamental epigenetic mechanism underlying eukaryotic gene regulation, yet little is known about how the catalytic activities of histone demethylases are regulated. Here, we identify and characterize NPAC/GLYR1 as an LSD2/KDM1b-specific cofactor that stimulates H3K4me1 and H3K4me2 demethylation. We determine the crystal structures of LSD2 alone and LSD2 in complex with the NPAC linker region in the absence or presence of histone H3 peptide, at resolutions of 2.9, 2.0, and 2.25 Å, respectively. These crystal structures and further biochemical characterization define a dodecapeptide of NPAC (residues 214–225) as the minimal functional unit for its cofactor activity and provide structural determinants and a molecular mechanism underlying the intrinsic cofactor activity of NPAC in stimulating LSD2-catalyzed H3K4 demethylation. Thus, these findings establish a model for how a cofactor directly regulates histone demethylation and will have a significant impact on our understanding of catalytic-activity-based epigenetic regulation.

[*]Correspondence: xuyh@fudan.edu.cn (Y.X.), yujiang_shi@hms.harvard.edu (Y.G.S.).
[8]These authors contributed equally to this work

ACCESSION NUMBERS The atomic coordinates of the structures in this work have been deposited in the Protein Data Bank with accession codes 4GU1 for LSD2, 4GUT for LSD2-NPAC, 4GUR for LSD2-NPAC-H3 (1–20; Space Group $p2_1$), and 4GUS for LSD2-NPAC-H3(1–20; Space Group $p3_221$).

SUPPLEMENTAL INFORMATION Supplemental Information includes six figures, four tables, and Supplemental Experimental Procedures and can be found with this article online at http://dx.doi.org/10.1016/j.molcel.2012.11.019.

INTRODUCTION

Since the discovery of the first histone-lysine-specific demethylase, LSD1/KDM1a, histone-lysine demethylation has emerged as an epigenetic paradigm (Shi et al., 2004). Thus far, over 20 histone-lysine demethylases (KDMs) have been characterized, belonging to either the flavin adenine dinucleotide (FAD)-dependent LSD family or the Fe^{2+} and α-ketoglutarate-dependent Jumonji C-terminal domain family (Allis et al., 2007; Bernstein et al., 2007; Chen et al., 2006b; Tsukada et al., 2006; Rice and Allis, 2001; Ruthenburg et al., 2007). Genetic, biochemical, and functional studies further indicate that these KDMs play crucial roles in a wide range of biological processes, including gene expression, cell growth, differentiation, development, and disease pathogenesis (Bhaumik et al., 2007; Egger et al., 2004; Esteller, 2008; Nottke et al., 2009; Shi, 2007).

A key question remains in the mechanistic understanding of precisely how the enzymatic activities of KDMs are regulated (Chen et al., 2006b; Horton et al., 2010; Lan et al., 2008; Wilson, 2007). It has been observed that many KDMs, although being active on synthetic peptides or core histone substrates, exhibit very weak or no detectable activity on nucleosomal substrates in vitro. When transfected into cells, however, robust activity on chromatin can be detected, suggesting the existence of additional cofactors required for full activity (Shi et al., 2004; Tahiliani et al., 2007). We, and others, have identified CoREST as a cofactor required for LSD1 action on nucleosomal substrates (Lee et al., 2005; Shi et al., 2005), representing the first break-through toward an understanding of how KDM activity is regulated. However, the molecular details underlying the cofactor-enhanced demethylase activity of LSD1 remain elusive (Forneris et al., 2007; Yang et al., 2006). Moreover, the cofactor activity of CoREST is highly specific, facilitating only demethylation of nucleosomal substrates by LSD1, but not any other KDMs. Further investigation is required for determining whether cofactor modulation is a general mechanism for the regulation of KDM functions. In particular, there are two areas to be addressed: first, whether different cofactors exist for other histone demethylases; and second, the molecular mechanism(s) employed by such cofactors to facilitate histone demethylase activity.

LSD2/KDM1b/AOF1 is the only mammalian ortholog of LSD1 and possesses similar histone H3K4 demethylase activity (Ciccone et al., 2009; Fang et al., 2010; Yang et al., 2010). However, LSD2 is a component of a different cellular complex and has functions distinct from those of LSD1 (Ciccone et al., 2009; Fang et al., 2010; van Essen et al., 2010). Genetic studies indicate that LSD2 is required for the homeostasis of global H3K4 methylation in mouse oocytes and regulates maternal gene imprinting (Ciccone et al., 2009). In somatic tissue, LSD2 seems to play an important role in active gene transcription. LSD2 is reported to be a potential H3K9 demethylase and is required for controlling NF-κB-induced gene activation by demethylating H3K9 at promoters (van Essen et al., 2010). On the other hand, we show that LSD2 is an active H3K4 demethylase that specifically associates with the coding region of target genes. Removal of endogenous LSD2 promotes an increase in H3K4me2 levels and a concurrent decrease in H3K9me2 levels specifically at coding regions, but not at the corresponding promoters, and results in downregulation of gene transcription (Fang et al., 2010). These genetic and functional studies suggest that LSD2 is an important epigenetic regulator involved in diverse biological processes. How LSD2 activity is targeted to various functional sites and whether its activity is regulated by specific cofactors remain unknown.

Here, we report a cofactor of LSD2, NPAC/GLYR1, which positively regulates H3K4me2- and H3K4me1-specific histone demethylase activity of LSD2. NPAC, a putative H3K36me3 reader (Vermeulen et al., 2010), is a previously uncharacterized integral component of the LSD2 histone demethylase complex (Fang et al., 2010). We show that NPAC directly

interacts with LSD2 and positively regulates its H3K4 demethylation activity both in vitro and in vivo. To understand the precise molecular mechanism of NPAC in regulating LSD2 enzymatic activity, we determined the crystal structures of LSD2, LSD2 in complex with NPAC, and the ternary complex of LSD2-NPAC-H3 peptide. These structural studies, together with molecular and biochemical characterization, illustrate a molecular model of cofactor-mediated regulation of the catalytic activity of a histone demethylase.

RESULTS

NPAC Is a Cofactor of LSD2 Positively Regulating Its H3K4 Histone Demethylase Activity

NPAC/GLYR1 (UniProtKB/Swiss-Prot ID: Q49A26) contains multiple functional domains, including a PWWP (Pro-Trp-Trp-Pro) domain, an AT-hook motif, and a dehydrogenase domain (Figure 1A). The presence of a dehydrogenase domain within NPAC was particularly intriguing because CtBP, a well-known corepressor and component of the LSD1 complex, also possesses a dehydrogenase domain (Chinnadurai, 2007; Shi et al., 2003). The potential analogy of NPAC/LSD2 to CtBP/LSD1 prompted us to focus on understanding the activity of NPAC in relation to LSD2 function. However, unlike CtBP, attempts to identify the intrinsic enzymatic activity of NPAC as a potential dehydrogenase using either recombinant NPAC protein purified from *E. coli* or the NPAC complex purified from HeLa cells via tandem affinity purification (TAP) were unsuccessful (data not shown).

Although no intrinsic histone demethylase activity was observed for recombinant NPAC, we did observe that the NPAC complex purified from HeLa cells via TAP has robust H3K4me2 demethylase activity toward nucleosomes (Figure 1B, lane 1). The H3K4 demethylase activity of the NPAC complex is probably attributable to endogenous LSD2, given that LSD2 was the only histone demethylase detected in the complex by mass spectrometry (MS; data not shown). Paradoxically, although the H3K4 demethylase activity was higher, the relative amount of LSD2 in the NPAC complex was significantly lower than that of the LSD2 complex, in which a small amount of endogenous NPAC was copurified with LSD2 (Figure 1Bg). The addition of purified recombinant NPAC to the LSD2 complex significantly increased nucleosomal demethylation (Figure 1C). These observations suggest that NPAC may positively regulate LSD2 histone demethylase activity on nucleosomes, similar to the cofactor activity of CoREST for LSD1 (Lee et al., 2005; Shi et al., 2005).

To directly validate its cofactor activity, we investigated whether NPAC alone is sufficient to enhance the activity of recombinant LSD2 in vitro. We have previously reported that, unlike LSD1, recombinant LSD2 can demethylate nucleosomal H3K4me2 at a high dosage (Fang et al., 2010). Therefore, to measure the stimulatory effect of NPAC on nucleosomal substrates, we titrated down the amount of recombinant hexa-His-tagged LSD2 (His-LSD2) until no obvious histone demethylase activity was detected (Figure S1A, lane 5, available online). Using this threshold dosage of His-LSD2, we performed nucleosome demethylation assays with increasing amounts of recombinant His-NPAC, which stimulated LSD2 activity in a dose-dependent manner (Figure 1D). In contrast, NPAC has no stimulatory effect on nucleosome demethylation by LSD1 (Figure S1B), and NPAC itself possesses no demethylase activity (Figure 1D, lane 9).

To further validate NPAC cofactor function in vivo, we coexpressed NPAC and LSD2, and we observed a much more pronounced depletion of di- and monomethylated H3K4 in cells than when expressing LSD2 alone (Figures 1E and S1C). Coexpression of NPAC does not change the substrate specificity of LSD2, because H3K9me2 and other histone marks examined showed no detectable changes (Figure S1D and data not shown). Taken together, both in vitro and in vivo data suggest that NPAC is a specific cofactor for LSD2, positively regulating its H3K4-specific histone demethylase activity.

The Linker Region of NPAC Is Sufficient for Cofactor Activity and LSD2 Interaction

To identify the functional domain responsible for NPAC cofactor activity, we generated NPAC deletion mutants (Figure 2A) and examined their abilities to facilitate LSD2 activity on nucleosome substrates. Neither the PWWP domain (NP.d1, residues 1–150) nor the dehydrogenase domain (NP.d5, residues 262–553) stimulated LSD2 (Figure 2B, lanes 5 and 9 compared to lanes 2 and 11). In contrast, truncation proteins containing the linker region, NP.d2 (residues 1–252), NP.d3 (residues 152–252), and NP.d4 (residues 152–553), significantly enhanced LSD2 demethylase activity (lanes 6–8), whereas deletion of the linker region (residues 152–252) abolished cofactor activity (NP.d6, lane 10). Furthermore, the linker region of NPAC exhibits strong cofactor activity for LSD2 when a synthetic H3K4me2 peptide (residues 1–21) is used as the substrate (Figure 2C).

Examining the same NPAC mutants using glutathione S-transferase (GST)-pull-down assays, we further showed that truncation proteins possessing strong cofactor activity (NP.d2, NP.d3, and NP.d4) are also capable of directly interacting with LSD2 (Figure 2D). Neither the PWWP domain (NP.d1) nor the dehydrogenase domain (NP.d5) interacted with LSD2 (lanes 4 and 8, respectively), and removal of either domain (NP.d4 or NP.d2) did not adversely affect LSD2 binding (lanes 7 and 5, compared to lane 3). Removing the linker region (NP.d6) abolished NPAC-LSD2 interaction (lane 9).

Taking these results together, we conclude that the linker region of NPAC is responsible for LSD2 interaction as well as for cofactor activity. It has been proposed that CoREST stimulates LSD1 histone demethylase activity on nucleosomes by assisting in the docking of LSD1-CoREST to nucleosomal substrates via its DNA-binding SANT2 domain (Yang et al., 2006). In contrast, the linker region of NPAC facilitates LSD2 enzymatic activity, regardless of whether the substrate is chromatin, nucleosome, or a modified short histone peptide, and the nucleosome-binding PWWP domain of NPAC is dispensable for its cofactor activity. These observations suggest a mechanism for the direct action of a cofactor on histone demethylation, not depending on the nucleosomal context, but primarily involving the histone tail.

The Crystal Structures of LSD2, LSD2-NPAC, and the Ternary Complex of LSD2-NPAC-H3 Peptide

To understand the structural basis for LSD2 function and its regulation by NPAC, we solved the LSD2 crystal structure using a truncated protein (residues 51–822) purified to homogeneity, as well as the cocrystal structures of LSD2 in complex with the NPAC linker region (amino acids 152–268) in the presence and absence of H3K4M peptides (Histone H3 residues 1–21, replacing K4 with a methionine to mimic the H3K4me2 substrate of LSD2) (Forneris et al., 2007). Resolutions of the refined models were 2.9 Å, 2.25 Å, and 2.0 Å, respectively (Table 1, Table S1, and Figure S2).

The structure of LSD2 adopts a compact rod shape and comprises four recognizable domains: a zinc-finger domain with two zinc atoms coordinated by a $Cys_4His_2Cys_2$ motif (ZF, lime), a CW-type zinc-finger domain with one zinc atom coordinated by four cysteines (Zf-CW, purple), a SWIRM domain (red), and an amine oxidase domain (AO, green) (Figures 3A and 3B). Compared to the structure of LSD2 alone, the cocrystal structures show that NPAC binding does not significantly alter the overall structure of LSD2 or induce conformational changes in the catalytic domain. Similarly, the inclusion of histone H3K4M peptide does not lead to significant conformational changes in the LSD2-NPAC complex (Figures 3C, 3D, and S3A and Table S2). This suggests that, unlike regulators of the SET1-family histone methyltransferases (Dou et al., 2006; Southall et al., 2009), NPAC does not

employ an allosteric mechanism to facilitate LSD2 enzymatic activity or switch LSD2 substrate specificity (Figures S3B and S3C).

The LSD2 Structure Reveals Features Common with and Distinct from LSD1

LSD2 and LSD1 share significant similarities in the AO catalytic domain (Chen et al., 2006a; Forneris et al., 2007; Stavropoulos et al., 2006; Yang et al., 2006). The overall folding and positions of the catalytic residue K661 and residues coordinating the FAD coenzyme are well conserved, creating indistinguishable catalytic cavities (Figures S4A–S4C), consistent with their similar substrate specificities (Ciccone et al., 2009; Fang et al., 2010; Shi et al., 2004; Yang et al., 2010). However, the crystal structure reveals several distinctive structural features of LSD2, which may significantly influence its intrinsic histone demethylase activity and explain differing regulatory mechanisms.

The most striking structural difference between LSD2 and LSD1 is the “tower domain,” which is present in the LSD1 AO domain but absent in LSD2 (Figure 4A). The tower domain of LSD1 is the binding site for CoREST. The lack of a tower domain in LSD2 inherently necessitates an alternate mechanism for LSD2-cofactor interaction. Another distinction is that the two zinc-finger domains present in LSD2 are absent in LSD1 (Figures 4B and 4C). The first zinc finger of LSD2 bears little sequence or structural similarity to $Cys_4His_2Cys_2$-type or other types of zinc fingers in the Protein Data Bank. Notably, the Zf-CW domain of LSD2 superimposes with that of ZCWPW1 (Figure S4D), a specific reader of trimethyl H3K4 (Figure S4E)(He et al., 2010). However, the hydrophobic pocket in the LSD2 Zf-CW domain is filled with the side chain of residues L340 and I343 in the adjacent SWIRM domain (Figure S4F). Thus, it is unlikely to interact with other proteins or histone modifications on this surface unless significant conformational change occurs. In LSD2, the two zinc fingers wrap around the SWIRM domain and together form a globular structure that contacts the AO domain. Though the molecular function of these zinc fingers is unclear and warrants future investigation, both are required for LSD2 histone demethylase activity (Fang et al., 2010; Yang et al., 2010). These zinc fingers may play a structural role in stabilizing the conformation of the AO and SWIRM domains. In comparison, the N-terminal region of LSD1 is unstructured and dispensable for LSD1 activity (Shi et al., 2004). Finally, despite some similarities, a significant difference in the LSD2 SWIRM domain is an extended coiled loop connected to the α9-helix, whereas the corresponding region in LSD1 is a short α-helix (Figure 4D). This extended loop and the α9-helix are adjacent to the AO domain, suggesting a possible function in LSD2 enzymatic activity. Indeed, replacing the extended coil loop (residues 273–278) with a flexible peptide sequence (GSGSGS) significantly impaired its enzymatic activity in histone peptide demethylation assays (Figure 4E).

A Dodecapeptide of NPAC Interacts with LSD2

In the cocrystal structures, we unambiguously identified a dodecapeptide of NPAC (residues 214–225) (Figure S2B), whereas other residues of NPAC were not built into the final model due to lack of electron density. This short NPAC peptide binds to LSD2 in a deep hydrophobic groove located between the AO and SWIRM domains, close to its catalytic site (Figure 5A). Specifically, residues H219, F220, L221, and L222 of NPAC are deeply buried in the hydrophobic patch formed by residues L282, V284, L291, L361, F801, and L810 of LSD2 (Figure 5B). Residues 214–217 of NPAC are projected away from this hydrophobic patch and make little contact with LSD2. Notably, LSD2 residues L282, V284, and L291 are located in the α9-helix and in the upstream coiled loop of the LSD2 SWIRM domain, which is one of the structural differences from LSD1 (Figures 5C and S5A), and their conformation is nearly identical to the structure of LSD2 alone (Figures 4D and S3A).

To validate the importance of the dodecapeptide for NPAC-LSD2 interaction, we designed truncation mutants in the NPAC linker region (NP.d7–NP.d9, schematic shown in Figure 5D) and examined their ability to interact with LSD2 (Figure 5E). As expected, deletion of amino acids 214–222 from NP.d3 (NP.d9) completely abolished LSD2 binding (lane 6). NP.d8 (residues 188–252, lane 5), but not NP.d7 (residues 152–186, containing the AT-hook motif, lane 4), was sufficient for LSD2 interaction. Consistent with the results from these binding assays, NP.d8, but not NP.d7 or NP.d9, significantly enhanced LSD2 histone demethylase activity on nucleosomal substrates (Figure 5F). The cocrystal structures predict that residues H219, F220, L221, and L222 of NPAC form the major binding sites for LSD2. Indeed, point mutation and deletion of these critical residues within NPAC 188–252 (NP.M1– NP.M3, partial sequences shown in Figure 5G) result in the loss of LSD2 binding (Figure 5H), as well as the loss of the ability to stimulate LSD2 activity (Figure 5I). Collectively, these results confirm the structural predictions and identify the key residues of NPAC whose interaction with LSD2 is important for NPAC cofactor activity.

Interplay among Enzyme, Cofactor, and Substrate

Despite similar interactions observed between the N terminus of the H3 peptide and the catalytic cavity of LSD2 and LSD1 (Figures S4A–S4C), the cocrystal structure of the LSD2-NPAC-H3 peptide complex reveals additional, unique interactions among enzyme, cofactor, and substrate (summarized in Figure S5). A network of hydrogen bonds is formed between the main chains of K18 and L20 of H3K4M peptide and G279, E277, and N276 of LSD2, and between the side chains of H3Q19 and N276 of LSD2 (Figures 6A and 6B). These interactions are unique to LSD2; they are not observed in the cocrystal structure of the ternary complex of LSD1, CoREST, and an H3K4M peptide, in which only residues 1–16 of histone H3 are visible (Forneris et al., 2007). We speculate that the interactions between H3 substrate and LSD2 residues in the extended loop may explain why this region is important for its enzymatic activity (Figure 4E).

The structure of the ternary complex also reveals a unique interaction of H3 peptide with the LSD2-NPAC complex. NPAC F217, together with LSD2 residues Y273, E277, and R285, creates a new hydrophobic patch in the LSD2-NPAC complex that accommodates the side chain of H3L20 (Figure 6C), suggesting a stronger substrate interaction compared to LSD2 alone. In the cocrystal structure, the side chain of H3K18 is in close proximity to D214 and H216 of NPAC, suggesting potential contacts. However, the electron density of the side chain of H3K18 is weak (Figure S2A), suggesting a flexible conformation and weak interactions involving the H3K18 side chain. Taken together, these structural analyses suggest that the dodecapeptide (NPAC residues 214–225) is the minimal functional unit for NPAC cofactor activity. The residues H219, F220, L221, and L222 of NPAC form the major binding sites for LSD2 and are responsible for LSD2 and NPAC interaction, whereas NPAC residue F217 probably contributes directly to the cofactor activity of NPAC by stabilizing the enzyme-substrate complex.

F217 of NPAC Stabilizes Enzyme-Substrate Interaction and Is Essential for Cofactor Activity

To determine whether the dodecapeptide (NPAC residues 214–225) is the minimal functional unit for NPAC cofactor activity and whether F217 plays a critical role, we synthesized the wild-type and mutant dodecapeptides and examined their cofactor activities (NP.M4– NP.M6, sequences shown in Figure 6D). As expected, wild-type NPAC peptide is sufficient to enhance LSD2 activity in nucleosome demethylation assays (Figure 6E, comparing lane 3 to lane 2), whereas the F217A single mutation (NP.M6) abolishes cofactor activity (lane 6). In contrast, mutations of D214 and H216 (NP.M4 and NP.M5) have a marginal effect on cofactor activity (comparing lanes 4 and 5 to lane 6), consistent with the

structural predictions that neither residue makes important contacts with LSD2 or H3 peptide. These results were further confirmed in demethylation assays using H3K4me2 peptide substrate (residues 1–21) (Figure 6F).

We did not detect NPAC cofactor activity when a shorter H3K4me2 peptide (residues 1–15) was used, even though weak demethylation activity of this substrate was detected using a high concentration of LSD2 (Figures S6A and S6B). This result supports our model that H3L20 is important for NPAC cofactor activity in making contact with the LSD2-NPAC complex. The significant differences between H3K4me2 peptides 1–15 and 1–21 suggest that the length of the H3 peptide may affect LSD2 enzymatic activity, thus potentially influencing NPAC cofactor activity. To investigate this further, we synthesized a longer H3K4me2 peptide (H3 residues 1–44). Interestingly, the longer peptide seems to be a better substrate for LSD2. Under identical conditions, LSD2 demethylated a large majority of the longer H3K4me2 peptide (1–44), producing H3K4me1 and also H3K4me0 products, whereas only around 30% of H3K4me2 of the short peptide (1–21) was converted to H3K4me1. These observations indicate that H3 residues 16–44 may interact with LSD2 outside its catalytic cavity and that these interactions significantly influence H3K4 demethylation efficiency. Notably, the wild-type NPAC protein can robustly stimulate LSD2 demethylation of the longer peptide (1–44), and the cofactor activity of F217A NPAC mutant was very weak or undetectable (Figure S6C).

To further characterize the importance of NPAC F217 for cofactor activity, we compared full-length wild-type and F217A NPAC protein in nucleosome demethylation assays. Using a threshold amount of LSD2 where no obvious nucleosome demethylase activity was observed (Figure S6D, lanes 2 and 9), we did not detect cofactor activity of the F217A mutant, whereas wild-type NPAC showed robust activity (Figure S6D, lanes 10–14). However, residual stimulatory activity of full-length NPAC F217A protein was detected when more NPAC and LSD2 proteins were used (Figure S6Ea, lanes 4 and 9). Wild-type NPAC clearly has a cofactor activity far superior to that of the F217A mutant (Figures S6Db and S6Eb, comparing lanes 3 versus 4 and 8 versus 9). This demonstrates the central role of F217 in NPAC cofactor activity and emphasizes the importance of the interactions of the H3 tail along the surface of the LSD2 enzyme to demethylase activity.

To investigate the functional role of NPAC F217 in its cofactor activity, we first examined the effect of the F217A mutation on LSD2 binding. Isothermal titration calorimetry (ITC) studies showed that wild-type, F217A, and D214A/H216A/F217A triple mutant peptides bind to LSD2 equally well, with a binding affinity (Kd) of 0.92 ± 0.08 μM, 0.93 ± 0.07 μM, and 0.99 ± 0.08 μM, respectively (Figure 6G and Table S3). Thus, the side chains of NPAC residues F217, D214, and H216 are not involved in LSD2 interaction, consistent with the structural predictions. Importantly, the result demonstrates that the inactivation of NPAC F217A mutant is not due to compromised LSD2 interaction.

Next, we investigated the effect of wild-type and mutant NPAC dodecapeptides on LSD2-H3K4M peptide binding via ITC. Shown in Figure 6H, H3K4M peptide had a higher affinity to the LSD2-NPAC complex (blue line) than to LSD2 alone (red line). Importantly, the F217A mutation (NP.M6) significantly diminished the ability of NPAC to stabilize the interaction between LSD2 and the H3K4M peptide (green line). Wild-type NPAC peptide had no appreciable affinity to the H3K4M peptide (cyan line). The thermodynamic features of these interactions are summarized in Table S4. Taken together, these results confirm that NPAC residue F217 directly contributes to the cofactor activity of NPAC by stabilizing the enzyme-substrate complex.

DISCUSSION

The present study identifies NPAC/GLYR1 as a cofactor specific for the LSD2/KDM1b histone demethylase. Our structural and biochemical studies have determined the minimal functional segment of NPAC (a dodecapeptide, residues 214–225) responsible for its cofactor activity. NPAC residues 219–223 interact directly with LSD2. This interaction aligns NPAC residue F217 with the hydrophobic patch on the surface of LSD2, creating a new binding pocket that accommodates the side chain of L20 on histone H3. As a result, NPAC stabilizes the interaction between LSD2 and histone H3 substrates, facilitating H3K4 demethylation. This study thus provides a detailed molecular model precisely illustrating a mechanism of cofactor-assisted histone demethylation.

Histone demethylases may associate with transcriptional factors or chromatin binding proteins and sometimes may themselves contain chromatin-binding modules. All of these present important mechanisms in targeting histone demethylases to specific loci that may consequently increase local enzyme concentration and facilitate histone demethylation. The proposed mechanism for LSD1 cofactor CoREST fits this model (Yang et al., 2006). As a putative H3K36me3 binding protein, NPAC may also play an important role in targeting LSD2 in the human genome. However, independent of its PWWP chromatin-binding module, an NPAC dodecapeptide (residues 214–225) shows robust cofactor activity, stimulating LSD2 demethylation of both nucleosomes and synthetic histone peptides. Thus, we show a cofactor activity independent of the targeting effect, challenging the dogma of histone demethylase regulation.

Our finding answers an intriguing question: What happens beyond the tethering of a histone demethylase to nucleosomes? We propose that the interactions of the H3 tail with LSD2 outside of its catalytic cavity play an important role in regulating histone demethylation efficiency. Structural and biochemical data indicate that NPAC cofactor activity is centered on residue F217 and its ability to assist LSD2 interacting with histone H3L20. The effect of this single interaction on LSD2 activity is striking considering the extensive interactions already in place, particularly between histone H3 residues 1–16 and the LSD2 catalytic domain (Figure S5B). It suggests that even weak interactions of the H3 tail along the surface of the enzyme can be important. Indeed, we observed that LSD2 prefers longer H3K4me2 peptides (Figures S6A–S6C). LSD1 shows no activity to H3K4me1 peptide 1–16, but can demethylate peptides 1–21 and 1–30 with similar efficiency (Forneris et al., 2005). Thus, H3 residues 17–21 are important for LSD1 demethylase activity even though the interaction was observed in the cocrystal structure (Forneris et al., 2007; Yang et al., 2006). We speculate that stabilizing the interaction between the H3 tail and histone demethylases, either by protein factors similar to NPAC or by additional histone modifications on the H3 tail, may present an important mechanism in regulating histone demethylase activity.

Though CoREST may contribute to cofactor activity for LSD1 through a docking mechanism, there are at least two pieces of evidence indicating additional mechanisms exist. We and others have shown that the CoREST linker region without the two SANT domains retains significant cofactor activity for LSD1 (Lee et al., 2005; Shi et al., 2005). Moreover, Forneris and colleagues showed that CoREST-bound LSD1 exhibits a 2-fold increase in catalytic rate using H3K4me2 peptide substrate (residues 1–21) (Forneris et al., 2007). Our findings presented here with NPAC and LSD2 provide a plausible mechanism to be explored in the context of CoREST and LSD1.

Findings from the present study have significantly advanced our current understanding of cofactor-mediated regulation of histone lysine demethylases in many other aspects. Our findings suggest that the regulation of the enzymatic activity by associated cofactors is

probably a general mechanism underlying the regulation of KDM function. Also, the high selectivity of cofactors for histone demethylases, with each cofactor preferentially and specifically regulating its associated KDM, but not the others, may have significant biological implications by defining their specific functional loci in the genome. The present study does not exclude the possibility that one common cofactor may work for several KDMs under certain circumstances; however, it is also possible that each KDM may have more than one cofactor to regulate its diverse functions in distinctive biological processes. For example, LSD1 is regulated by several associating factors besides CoREST, including BHC80 (Lan et al., 2007), MTA-2 (Wang et al., 2009), and nuclear receptors such as estrogen and androgen receptors (Metzger et al., 2005; Nair et al., 2010).

Of particular note, our biochemical and structural analyses suggest that NPAC facilitates H3K4-specific demethylase activity of LSD2 but does not promote switching to H3K9 demethylase activity. Similar to LSD1, the cocrystal structure reveals extensive interactions between the histone H3 tail and the enzyme. The side chain of H3K4M fits nicely in the catalytic site, consistent with the robust H3K4 demethylation activity. In contrast, the side chain of H3K9 is distant from the FAD N5 atom, making LSD2 unfavorable as a potential H3K9me1 or H3K9me2 demethylase (Figures S3B–S3C). However, mouse LSD2 has been reported to possess H3K9 demethylase activity (van Essen et al., 2010). Thus, it remains unclear how LSD2, and arguably also LSD1, might demethylate H3K9. Binding of NPAC does not induce conformational changes significant enough to allow the switch of LSD2 substrate selectivity (H3K4 versus H3K9, Figure S3). However, we do not exclude the possibility that binding of a yet-unidentified cofactor to LSD2 may significantly change its conformation, enabling H3K9 demethylation.

Finally, the findings from the present study have significant biological, clinical, and therapeutic implications. Abrogated expression or enzymatic activity of histone demethylases has been strongly implicated in human diseases such as cancer (Chi et al., 2010; Esteller, 2008; Smith et al., 2007). Therefore, deciphering the regulatory mechanisms of histone demethylases is crucial for understanding their biological and pathophysiological functions (Ng et al., 2007; Chen et al., 2006b; Horton et al., 2010; Shi, 2007). However, this area of research currently remains under investigation. Our study provides a potential foundation for the rational design of specific inhibitors or activators of histone demethylases based on their selective interaction with corresponding cofactors. This is significant, as most current LSD inhibitors effectively inhibit both LSD1 and LSD2 indiscriminately, which is not surprising given their nearly indistinguishable catalytic domains (Binda et al., 2010; Stavropoulos and Hoelz, 2007). Thus, these findings are valuable for future translational research toward epigenetic medicines.

EXPERIMENTAL PROCEDURES

Crystallization and Data Collection

All crystals were grown using the hanging-drop vapor diffusion method. LSD2 (residues 51–822) and NPAC (residues 152–268) were used. The LSD2 used for crystallization of the enzyme alone contains N-terminal extra residues (PLGSEFKGLRRR), whereas the LSD2 used for other crystallization contains extra residues (GPGS) that result from 3C cleavage. The H3 peptide used for crystallization is ARTMQTARKSTGGKAPRKQLA (H3K4M, residues 1–21). Crystals of LSD2 alone were grown in conditions with reservoir containing 7% polyethylene glycol (PEG) 8000, 200 mM NaCl, and 100 mM Na_2HPO_4-KH_2PO_4 (pH 6.0) at 18°C. The LSD2-NPAC complex was grown in conditions with buffer consisting of 10% PEG 3350, 20 mM citric acid, and 30 mM Bis-tris propane at 4°C. The LSD2-NPAC-H3K4M complex was crystallized in two forms. One belongs to space group $P2_1$ in conditions with reservoir containing 10% PEG 3350, 20 mM citric acid, and 30 mM Bis-tris

propane, and the other belongs to space group $P3_221$ in conditions with reservoir containing 10% PEG 3350, 100 mM NH_4I, and 100 mM MES (pH 6.2) at 4°C (Table 1 and Table S1). All crystals were slowly equilibrated with a cryoprotectant buffer containing reservoir buffer plus 15% glycerol (v/v) and were flash frozen in a cold nitrogen stream at −173°C. All crystals were examined on an X8 PROTEUM system (Bruker AXS), and data sets were collected on beamline BL17U at the Shanghai Synchrotron Radiation Facility (SSRF, Shanghai, China). All data were processed using the program HKL-2000 (Otwinowski and Minor, 1997).

Structure Determination

The structure of LSD2 alone was determined by molecular replacement using the LSD1 structure (2V1D.PDB) as a searching model (Forneris et al., 2007) in $P2_12_12_1$ form. The crystals contain two molecules in one asymmetric unit. Rotation and translation function searches were performed with the program PHASER (McCoy et al., 2005). The structures of LSD2-NPAC and LSD2-NPAC-H3K4M were determined with the Fourier difference method, and the models were manually built with the Crystallographic Object-Oriented Toolkit (COOT) (Emsley and Cowtan, 2004). All refinements were performed using the refinement module phenix.refine of the PHENIX package (Adams et al., 2002). The model quality was checked with the PROCHECK program (Laskowski et al., 1993), which showed good stereochemistry according to the Ramachandran plot for all structures. The structure-similarity search was performed with the DALI Server (Holm et al., 2008), and structure superimposition was performed with COOT (Emsley and Cowtan, 2004). Even though the $Cys_4His_2Cys_2$ motif of the LSD2-Zf domain (residues 51–137) resembles AN1-type zinc fingers, its structure bears little similarity to AN1-Zfs or other zinc fingers in the PDB. All structure figures were generated with PyMOL (De-Lano, 2002). Statistics of the structure determination and refinement are summarized in Table 1 and Table S1.

Histone Demethylase Activity Assays

Histone peptides are purchased from Millipore or custom synthesized. The purity of all peptides is >95%, as determined by high-performance liquid chromatography and MS. In vitro histone demethylase activity assays were performed as described (Shi et al., 2004). In brief, purified LSD2 and NPAC-derived peptides or proteins were incubated with 50 μM H3K4me2 peptides (residues 1–21) in 50 mM Tris-HCl (pH 8.5), 50 mM KCl, 5 mM $MgCl_2$, and 5% glycerol at 37°C for 30 min. The products were desalted through a C18 Zip-tip (Millipore) and analyzed on a MALDI-TOF micro MX mass spectrometer (ABI 4700, Applied Biosystems). The laser intensity was kept constant for all of the samples. All MS data were processed using Data Explorer 4.5 (Applied Biosystems). Both full-length and truncated LSD2 (residues 51–822) were used for histone peptide demethylation assays, and similar results were obtained.

For nucleosome demethylation assays, typically 0.5 μg of full-length His-LSD2, 1 μg of NPAC protein or peptides, and 2 μg of nucleosomes purified from HeLa cells were used, and demethylation efficiency was analyzed by SDS-PAGE electrophoresis and immunoblot using methylation-specific histone H3 antibodies as previously described (Shi et al., 2004).

Supplementary Material

Refer to Web version on PubMed Central for supplementary material.

Acknowledgments

We thank staff members of beamline BL17U at SSRF for assistance in data collection and staff members of the Biomedical Core Facility, Fudan University for mass spectrometry analyses. We thank James Chou, Paco Kang,

and Lisa Schwartz for critical reading of the manuscript. This work was supported by grants from the National Institutes of Health (5R01GM078458) and Brigham and Women's Hospital Funds to Sustain Research Excellence to Y.G.S., and the National Basic Research Program of China (2011CB965300 and 2009CB918600), the National Natural Science Foundation of China (81130047, 31270779, 31030019, 11079016, and 30870493), and the Fok Ying Tung Education Foundation (20090071220012).

REFERENCES

Adams PD, Grosse-Kunstleve RW, Hung LW, Ioerger TR, McCoy AJ, Moriarty NW, Read RJ, Sacchettini JC, Sauter NK, Terwilliger TC. PHENIX: building new software for automated crystallographic structure determination. Acta Crystallogr. D Biol. Crystallogr. 2002; 58:1948–1954. [PubMed: 12393927]

Allis CD, Berger SL, Cote J, Dent S, Jenuwien T, Kouzarides T, Pillus L, Reinberg D, Shi Y, Shiekhattar R, et al. New nomenclature for chromatin-modifying enzymes. Cell. 2007; 131:633–636. [PubMed: 18022353]

Bernstein BE, Meissner A, Lander ES. The mammalian epigenome. Cell. 2007; 128:669–681. [PubMed: 17320505]

Bhaumik SR, Smith E, Shilatifard A. Covalent modifications of histones during development and disease pathogenesis. Nat. Struct. Mol. Biol. 2007; 14:1008–1016. [PubMed: 17984963]

Binda C, Valente S, Romanenghi M, Pilotto S, Cirilli R, Karytinos A, Ciossani G, Botrugno OA, Forneris F, Tardugno M, et al. Biochemical, structural, and biological evaluation of tranylcypromine derivatives as inhibitors of histone demethylases LSD1 and LSD2. J. Am. Chem. Soc. 2010; 132:6827–6833. [PubMed: 20415477]

Chen Y, Yang Y, Wang F, Wan K, Yamane K, Zhang Y, Lei M. Crystal structure of human histone lysine-specific demethylase 1 (LSD1). Proc. Natl. Acad. Sci. USA. 2006a; 103:13956–13961. [PubMed: 16956976]

Chen Z, Zang J, Whetstine J, Hong X, Davrazou F, Kutateladze TG, Simpson M, Mao Q, Pan CH, Dai S, et al. Structural insights into histone demethylation by JMJD2 family members. Cell. 2006b; 125:691–702. [PubMed: 16677698]

Chi P, Allis CD, Wang GG. Covalent histone modifications—miswritten, misinterpreted and mis-erased in human cancers. Nat. Rev. Cancer. 2010; 10:457–469. [PubMed: 20574448]

Chinnadurai G. Transcriptional regulation by C-terminal binding proteins. Int. J. Biochem. Cell Biol. 2007; 39:1593–1607. [PubMed: 17336131]

Ciccone DN, Su H, Hevi S, Gay F, Lei H, Bajko J, Xu G, Li E, Chen T. KDM1B is a histone H3K4 demethylase required to establish maternal genomic imprints. Nature. 2009; 461:415–418. [PubMed: 19727073]

DeLano, WL. The PyMOL Molecular Graphics System. 2002. http://www.pymol.org

Dou Y, Milne TA, Ruthenburg AJ, Lee S, Lee JW, Verdine GL, Allis CD, Roeder RG. Regulation of MLL1 H3K4 methyltransferase activity by its core components. Nat. Struct. Mol. Biol. 2006; 13:713–719. [PubMed: 16878130]

Egger G, Liang G, Aparicio A, Jones PA. Epigenetics in human disease and prospects for epigenetic therapy. Nature. 2004; 429:457–463. [PubMed: 15164071]

Emsley P, Cowtan K. Coot: model-building tools for molecular graphics. Acta Crystallogr. D Biol. Crystallogr. 2004; 60:2126–2132. [PubMed: 15572765]

Esteller M. Epigenetics in cancer. N. Engl. J. Med. 2008; 358:1148–1159. [PubMed: 18337604]

Fang R, Barbera AJ, Xu Y, Rutenberg M, Leonor T, Bi Q, Lan F, Mei P, Yuan GC, Lian C, et al. Human LSD2/KDM1b/AOF1 regulates gene transcription by modulating intragenic H3K4me2 methylation. Mol. Cell. 2010; 39:222–233. [PubMed: 20670891]

Forneris F, Binda C, Vanoni MA, Battaglioli E, Mattevi A. Human histone demethylase LSD1 reads the histone code. J. Biol. Chem. 2005; 280:41360–41365. [PubMed: 16223729]

Forneris F, Binda C, Adamo A, Battaglioli E, Mattevi A. Structural basis of LSD1-CoREST selectivity in histone H3 recognition. J. Biol. Chem. 2007; 282:20070–20074. [PubMed: 17537733]

He F, Umehara T, Saito K, Harada T, Watanabe S, Yabuki T, Kigawa T, Takahashi M, Kuwasako K, Tsuda K, et al. Structural insight into the zinc finger CW domain as a histone modification reader. Structure. 2010; 18:1127–1139. [PubMed: 20826339]

Holm L, Kääriäinen S, Rosenström P, Schenkel A. Searching protein structure databases with DaliLite v.3. Bioinformatics. 2008; 24:2780–2781. [PubMed: 18818215]

Horton JR, Upadhyay AK, Qi HH, Zhang X, Shi Y, Cheng X. Enzymatic and structural insights for substrate specificity of a family of jumonji histone lysine demethylases. Nat. Struct. Mol. Biol. 2010; 17:38–43. [PubMed: 20023638]

Lan F, Collins RE, De Cegli R, Alpatov R, Horton JR, Shi X, Gozani O, Cheng X, Shi Y. Recognition of unmethylated histone H3 lysine 4 links BHC80 to LSD1-mediated gene repression. Nature. 2007; 448:718–722. [PubMed: 17687328]

Lan F, Nottke AC, Shi Y. Mechanisms involved in the regulation of histone lysine demethylases. Curr. Opin. Cell Biol. 2008; 20:316–325. [PubMed: 18440794]

Laskowski RA, MacArthur MW, Moss DS, Thornton JM. PROCHECK: a program to check the stereochemical quality of protein structures. J. Appl. Cryst. 1993; 26:283–291.

Lee MG, Wynder C, Cooch N, Shiekhattar R. An essential role for CoREST in nucleosomal histone 3 lysine 4 demethylation. Nature. 2005; 437:432–435. [PubMed: 16079794]

McCoy AJ, Grosse-Kunstleve RW, Storoni LC, Read RJ. Likelihood-enhanced fast translation functions. Acta Crystallogr. D Biol. Crystallogr. 2005; 61:458–464. [PubMed: 15805601]

Metzger E, Wissmann M, Yin N, Müller JM, Schneider R, Peters AH, Günther T, Buettner R, Schüle R. LSD1 demethylates repressive histone marks to promote androgen-receptor-dependent transcription. Nature. 2005; 437:436–439. [PubMed: 16079795]

Nair SS, Nair BC, Cortez V, Chakravarty D, Metzger E, Schüle R, Brann DW, Tekmal RR, Vadlamudi RK. PELP1 is a reader of histone H3 methylation that facilitates oestrogen receptor-alpha target gene activation by regulating lysine demethylase 1 specificity. EMBO Rep. 2010; 11:438–444. [PubMed: 20448663]

Ng SS, Kavanagh KL, McDonough MA, Butler D, Pilka ES, Lienard BM, Bray JE, Savitsky P, Gileadi O, von Delft F, et al. Crystal structures of histone demethylase JMJD2A reveal basis for substrate specificity. Nature. 2007; 448:87–91. [PubMed: 17589501]

Nottke A, Colaiácovo MP, Shi Y. Developmental roles of the histone lysine demethylases. Development. 2009; 136:879–889. [PubMed: 19234061]

Otwinowski, Z.; Minor, W. Processing of X-ray Diffraction Data Collected in Oscillation Mode. In Methods in Enzymology. In: Carter, CW., Jr.; Sweet, RM., editors. Macromolecular Crystallography, part A. Vol. Volume 276. Academic Press; New York: 1997. p. 307-326.

Rice JC, Allis CD. Histone methylation versus histone acetylation: new insights into epigenetic regulation. Curr. Opin. Cell Biol. 2001; 13:263–273. [PubMed: 11343896]

Ruthenburg AJ, Allis CD, Wysocka J. Methylation of lysine 4 on histone H3: intricacy of writing and reading a single epigenetic mark. Mol. Cell. 2007; 25:15–30. [PubMed: 17218268]

Shi Y. Histone lysine demethylases: emerging roles in development, physiology and disease. Nat. Rev. Genet. 2007; 8:829–833. [PubMed: 17909537]

Shi Y, Sawada J, Sui G, Affar B, Whetstine JR, Lan F, Ogawa H, Luke MP, Nakatani Y, Shi Y. Coordinated histone modifications mediated by a CtBP co-repressor complex. Nature. 2003; 422:735–738. [PubMed: 12700765]

Shi Y, Lan F, Matson C, Mulligan P, Whetstine JR, Cole PA, Casero RA, Shi Y. Histone demethylation mediated by the nuclear amine oxidase homolog LSD1. Cell. 2004; 119:941–953. [PubMed: 15620353]

Shi YJ, Matson C, Lan F, Iwase S, Baba T, Shi Y. Regulation of LSD1 histone demethylase activity by its associated factors. Mol. Cell. 2005; 19:857–864. [PubMed: 16140033]

Smith LT, Otterson GA, Plass C. Unraveling the epigenetic code of cancer for therapy. Trends Genet. 2007; 23:449–456. [PubMed: 17681396]

Southall SM, Wong PS, Odho Z, Roe SM, Wilson JR. Structural basis for the requirement of additional factors for MLL1 SET domain activity and recognition of epigenetic marks. Mol. Cell. 2009; 33:181–191. [PubMed: 19187761]

Stavropoulos P, Hoelz A. Lysine-specific demethylase 1 as a potential therapeutic target. Expert Opin. Ther. Targets. 2007; 11:809–820. [PubMed: 17504018]

Stavropoulos P, Blobel G, Hoelz A. Crystal structure and mechanism of human lysine-specific demethylase-1. Nat. Struct. Mol. Biol. 2006; 13:626–632. [PubMed: 16799558]

Tahiliani M, Mei P, Fang R, Leonor T, Rutenberg M, Shimizu F, Li J, Rao A, Shi Y. The histone H3K4 demethylase SMCX links REST target genes to X-linked mental retardation. Nature. 2007; 447:601–605. [PubMed: 17468742]

Tsukada Y, Fang J, Erdjument-Bromage H, Warren ME, Borchers CH, Tempst P, Zhang Y. Histone demethylation by a family of JmjC domain-containing proteins. Nature. 2006; 439:811–816. [PubMed: 16362057]

van Essen D, Zhu Y, Saccani S. A feed-forward circuit controlling inducible NF-κB target gene activation by promoter histone demethylation. Mol. Cell. 2010; 39:750–760. [PubMed: 20832726]

Vermeulen M, Eberl HC, Matarese F, Marks H, Denissov S, Butter F, Lee KK, Olsen JV, Hyman AA, Stunnenberg HG, Mann M. Quantitative interaction proteomics and genome-wide profiling of epigenetic histone marks and their readers. Cell. 2010; 142:967–980. [PubMed: 20850016]

Wang Y, Zhang H, Chen Y, Sun Y, Yang F, Yu W, Liang J, Sun L, Yang X, Shi L, et al. LSD1 is a subunit of the NuRD complex and targets the metastasis programs in breast cancer. Cell. 2009; 138:660–672. [PubMed: 19703393]

Wilson JR. Targeting the JMJD2A histone lysine demethylase. Nat. Struct. Mol. Biol. 2007; 14:682–684. [PubMed: 17676028]

Yang M, Gocke CB, Luo X, Borek D, Tomchick DR, Machius M, Otwinowski Z, Yu H. Structural basis for CoREST-dependent demethylation of nucleosomes by the human LSD1 histone demethylase. Mol. Cell. 2006; 23:377–387. [PubMed: 16885027]

Yang Z, Jiang J, Stewart DM, Qi S, Yamane K, Li J, Zhang Y, Wong J. AOF1 is a histone H3K4 demethylase possessing demethylase activity-independent repression function. Cell Res. 2010; 20:276–287. [PubMed: 20101264]

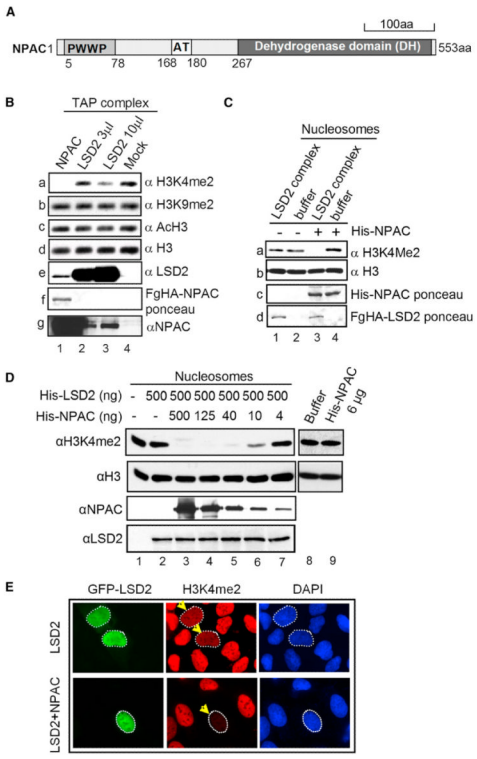

Figure 1. NPAC Is a Cofactor of LSD2 Positively Modulating Its H3K4 Demethylase Activity

(A) Schematic of NPAC domain structure. AT, AT-hook motif; PWWP, Pro-Trp-Trp-Pro domain.

(B) LSD2 in the NPAC complex can efficiently demethylate nucleosomal H3K4me2. Tandem-affinity-purified NPAC and LSD2 complexes were incubated with nucleosomes purified from HeLa cells and analyzed by immunoblot using the indicated antibodies.

(C) The addition of recombinant NPAC can improve H3K4 demethylase activity of the LSD2 complex.

(D) Recombinant NPAC stimulates LSD2 nucleosomal H3K4 demethylation in a dose-dependent manner. The amount of LSD2-enzyme and NPAC-cofactor proteins used in each reaction is indicated. Demethylation was assessed by immunoblot using the indicated antibodies. Significantly larger amounts of His-LSD2 are required for the efficient demethylation of nucleosomes (see Figure S1A).

(E) NPAC stimulates H3K4 demethylation mediated by LSD2 in cells. Immunofluorescence staining of U2OS transiently transfected with LSD2 alone or in combination with NPAC is shown. Green, GFP-LSD2; red, H3K4me2; blue, DAPI counterstain of DNA. Representatives with similar levels of GFP-LSD2 are shown. See also Figure S1.

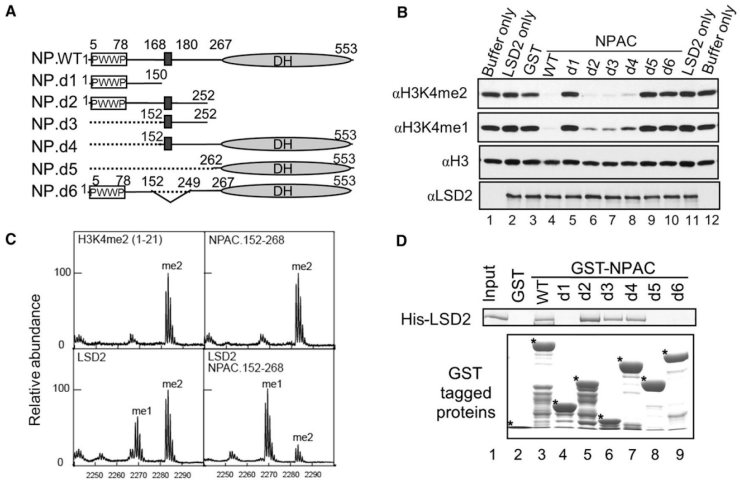

Figure 2. The Linker Region of NPAC Is Sufficient for Its Cofactor Activity and LSD2 Interaction

(A) Schematic representation of the wild-type and deletion mutants of NPAC. DH, dehydrogenase domain; black box, AT-hook motif.

(B) Nucleosome demethylation assays examining cofactor activities of NPAC mutants. Equal amounts of LSD2 were used in nucleosome demethylation reactions 2–11, in combination with various GST-tagged NPAC truncation proteins indicated above. GST was included as a negative control.

(C) The linker region of NPAC can stimulate LSD2 histone demethylase activity toward short H3K4me2 peptides. Molecular masses corresponding to mono- and dimethylated H3K4 peptides (residues 1–21) are denoted as me1 and me2, respectively.

(D) The linker region of NPAC is sufficient for LSD2 binding. Purified GST and GST-tagged wild-type and mutant NPAC proteins were used for GST pull-down of purified His-LSD2. Pull-down complexes were separated by SDS-PAGE and visualized by Coomassie blue staining. Asterisk, GST fusion protein.

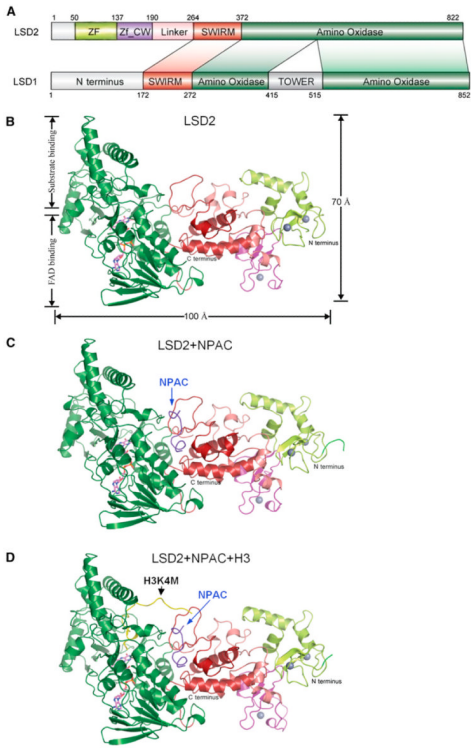

Figure 3. Binding of NPAC Does Not Induce Significant Conformational Changes in LSD2

(A) Comparison of the domain structures of human LSD2 and LSD1. Numbers indicate residue positions at the boundaries of each domain. The ZF domain is shown in lime, the Zf-CW domain in purple, the linker region in pink, the SWIRM domain in red, and the amine oxidase domain in green. The N-terminal flexible regions in both proteins and the tower domain of LSD1 are shown in gray. The same color scheme is used in all structural figures. (B–D) The crystal structures of LSD2 (B), NPAC-LSD2 heterodimer (C), and the ternary complex of LSD2-NPAC-H3 peptide (D). Disordered regions are shown in dashed lines, and FAD is shown in the stick representation (purple). Three zinc atoms are shown as gray balls. N and C termini of LSD2 are indicated. NPAC and H3K4M peptide are indicated and shown in the ribbon representation in blue and yellow, respectively. See also Figures S2 and S3 and Table S2.

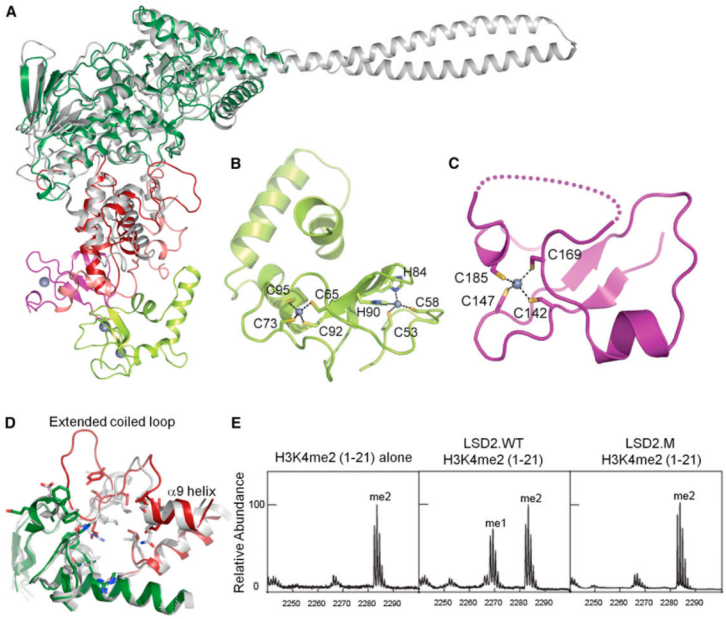

Figure 4. LSD2 Exhibits Both Common and Distinctive Structural Features Compared to LSD1

(A) Structural overlay of LSD2 (colored as in Figure 3) and LSD1 (gray).

(B) Structure of the N-terminal zinc finger of LSD2. Two zinc ions (gray balls) are coordinated with a $Cys_4His_2Cys_2$ motif with the indicated residues shown in stick representation. This zinc-finger domain bears little resemblance to known zinc-finger structures.

(C) Structure of the CW-type zinc finger of LSD2. Residues involved in zinc coordination are labeled and shown in stick representation. The disordered region is indicated by a dotted line.

(D) Superimposed structures of the SWIRM domains of LSD2 and LSD1, colored as in (A). The extended loop and α9-helix in LSD2 SWIRM domain are denoted. The side chains of unconserved residues are presented in stick presentation.

(E) Mutation of the extended loop in LSD2 SWIRM domain impairs its histone demethylase activity. MALDI-TOF MS analyses of the demethylation of H3K4me2 peptides incubated with the indicated proteins are shown. LSD2.WT, wild-type LSD2; LSD2.M, an LSD2 mutant replacing YQPNEC 273–278 with a flexible linker GSGSGS. See also Figure S4 and Table S2.

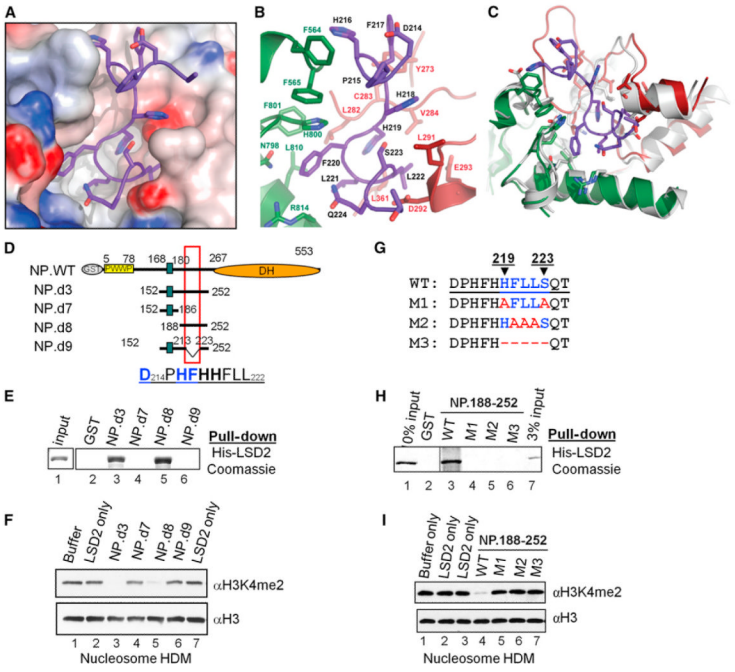

Figure 5. A Dodecapeptide of NPAC Interacts with LSD2

(A and B) Accommodation of NPAC residues in a hydrophobic pocket between the AO and SWIRM domains of LSD2. The surface rendering and ribbon representation of LSD2 are shown in (A) and (B), respectively. Critical residues involved in the interaction are shown in stick representation and colored in green (from the LSD2 AO domain), red (from the LSD2 SWIRM domain), and purple (from NPAC), respectively.

(C) Structural superimposition of the NPAC binding site of LSD2 and the corresponding regions of LSD1. The LSD2 structures are nearly identical with or without NPAC binding.

(D) Schematic of deletion mutants of the NPAC linker region (NP.d7–NP.d9). The red box marks the position of NPAC residues 214–225.

(E) Examination of LSD2 binding of NPAC deletion mutants by GST pull-down. His-LSD2 in pull-down products were separated by SDS-PAGE and visualized by Coomassie blue staining.

(F) Examination of the cofactor activity of NPAC mutants described in (D) using nucleosome demethylation assays. Immunoblots using the indicated antibodies are shown.

(G) Partial sequences of NPAC mutations (NP.M1–NP.M3, residues 188–252) disrupting the potential NPAC binding site for LSD2 interaction.

(H) GST-pull-down analyses of LSD2 binding by NPAC mutants in (G). Coomassie blue staining of His-LSD2 in input and GST-pull-down complexes is shown.

(I) Cofactor activity analyses of NPAC mutants described in (G) using nucleosomal demethylation assays.

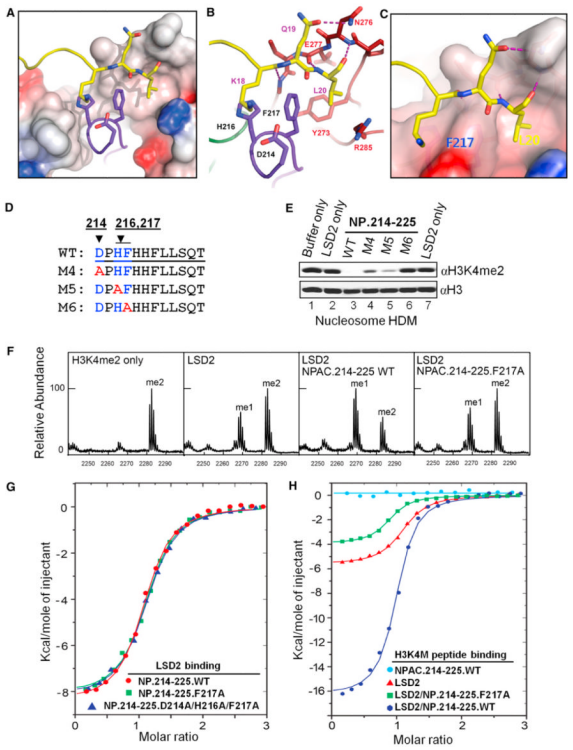

Figure 6. The NPAC Dodecapeptide Stimulates LSD2 Histone Demethylase Activity by Assisting Enzyme-Substrate Interaction

(A and B) A close-up view of the interplay of LSD2, NPAC, and H3K4M peptide in the cocrystal structure. The surface rendering and ribbon representation of LSD2 are shown in (A) and (B), respectively. H3K4M peptide (histone H3 residues 1–21, with Lys4 replaced with a Met) and NPAC (residues 214–225) are shown in the ribbon representation and colored in yellow and purple, respectively. Critical residues involved in H3 peptide interaction are shown in stick representation. Hydrogen bonds are indicated by dashed lines.

(C) H3L20 makes a new contact with the NPAC-LSD2 complex, with its side chain inserted in a hydrophobic patch formed by NPAC F217 and LSD2 residues.

(D) Sequences of wild-type (NP.WT) and mutant NPAC dodecapeptides (NP.M4–NP.M6) disrupting the potential interaction of NPAC with H3K4M peptide in the LSD2-NPAC-H3K4M peptide ternary complex.

(E) NPAC F217 is essential for its cofactor activity. Immunoblots of nucleosome demethylation assays are shown.

(F) The wild-type NPAC dodecapeptide, but not the F217A mutant, can stimulate LSD2-mediated demethylation of H3K4me2 peptides.

(G) Mutations of D214, H216, and F217 of NPAC do not affect LSD2 binding. ITC enthalpy plots of wild-type and mutant NPAC dodecapeptide binding to LSD2 are shown. Indicated NPAC peptides were injected into LSD2 containing cuvettes.

(H) ITC enthalpy plots of the binding of the H3K4M peptide to LSD2 and LSD2 in complex with either wild-type (WT) or F217A (M6) NPAC peptides (residues 214– 225). H3K4M peptide (residues 1–21) was injected into cuvettes containing the indicated combination of LSD2 and NPAC peptides. See also Figures S5 and S6 and Tables S3 and S4.

Table 1

Crystallographic Data and Structure Refinement Statistics

Data Collection			
Crystal (PDB ID code)	LSD2 (4GU1)	LSD2-NPAC (4GUT)	LSD2-NPAC-H3K4M(4GUS)[c]
Wavelength (Å)	0.97947	0.97916	1.00001
Resolution (Å)	50.00–2.90 (3.00–2.90)	50.00–2.00 (2.07–2.00)	50.00–2.25 (2.33–2.25)
Space group	$P2_12_12_1$	$P2_1$	$P3_221$
Cell parameters (Å, °)	*a* = 89.2 *b* = 89.2 *c* = 342.5	*a* = 62.0 *b* = 89.8 *c* = 86.7 β = 105.0°	*a* = 101.1 *b* = 101.1 *c* = 177.4 γ = 120.0°
Completeness (%)	99.5 (98.2)	95.2 (75.9)	99.9 (100.0)
R_{merge} (%)	12.4 (67.0)	7.6 (34.6)	8.1 (65.3)
I/σ (I)	17.4 (2.5)	23.5 (3.6)	24.6 (3.6)
Redundancy	13.5 (8.6)	6.8 (5.0)	10.6 (10.6)
No. of all reflections	785,997 (48,478)	402,920 (23,610)	548,052 (54,314)
No. of unique reflections	58,222 (5,637)	59,253 (4,722)	51,703 (5,124)
Refinement Statistics			
Resolution (Å)[a]	50.00–2.90 (3.00–2.90)	50.00–2.00 (2.07–2.00)	50.00–2.25 (2.33–2.25)
R_{work}/R_{free} (%)[b]	18.50/22.79	19.60/20.72	20.71/23.70
Deviation from Identity			
Bonds (Å)	0.011	0.011	0.008
Angles (°)	1.342	1.147	1.039
Average B factor (Å2)	83.438	39.159	44.413
Ramachandran Plot Statistics			
Most favored regions (%)	85.8	91.3	88.2
Allowed regions (%)	13.8	8.4	11.5
Generously allowed regions (%)	0.1	0	0
Disallowed regions (%)[d]	0.3	0.3	0.3

PDB, Protein Data Bank.

[a]The values for the data in the highest-resolution shell are shown in parentheses.

[b]R_{free} =∑Test||Fobs| –|Fcalc||/∑Test |Fobs|, where “Test” is a test set of about 5% of the total reflections randomly chosen and set aside prior to refinement for the complex.

[c] The LSD2-NPAC-H3K4M structure was also determined in the $P2_1$ crystal form, which is similar to the structure in $P3_221$ form (Tables S1 and S2).

[d] Residues Q803 and K75 of LSD2 lie in disallowed regions, and both residues locate at turn regions. The main chain of LSD2 Q803 interacts with FAD, and the side chain forms a hydrogen bond with the residues A546 and S768. Together, these strong interactions lead to a restrained conformation of Q803 of LSD2. A hydrogen-bond interaction is formed between LSD2 residues A74 and G77, which possibly distorts K75 and causes it to lie in a disallowed region.